

SUPPORTING INFORMATION

ALD of ZnO:Ti : growth mechanism and application as efficient transparent conductive oxide in silicon nanowire solar cells

*Damien Coutancier,^{1,2} Shan-Ting Zhang,^{1,2} Simone Bernardini,^{1,3} Olivier Fournier,^{1,4}
Tiphaine Mathieu-Pennober,⁵ Frédérique Donsanti,^{1,4} Maria Tchernycheva,⁵ Martin
Foldyna,⁶ Nathanaelle Schneider^{*,1,2}*

¹ Institut Photovoltaïque d'Ile-de-France (IPVF), 18 boulevard Thomas Gobert, 91120
Palaiseau, France

² CNRS, UMR 9006, Institut Photovoltaïque d'Ile-de-France (IPVF), 18 boulevard
Thomas Gobert, 91120 Palaiseau, France

³ TOTAL, 18 boulevard Thomas Gobert, 91120 Palaiseau, France

⁴ EDF R&D, IPVF, 18 boulevard Thomas Gobert, 91120 Palaiseau, France

⁵ Centre de Nanosciences et de Nanotechnologies, UMR 9001 CNRS, Univ. Paris-

Saclay, 10 Boulevard Thomas Gobert, 91120 Palaiseau Cedex, France.

⁶ LPICM, CNRS, Ecole Polytechnique, IP Paris, 91128 Palaiseau, France

Corresponding Author

*E-mail: n.schneider@cnrs.fr (N. Schneider)

Figure S1. Influence of the precursor introduction on the structural properties of ALD-TZO

films (sequence A : {ZnO} = H₂O pulse / N₂ purge / DEZ pulse / N₂ purge ; sequence B

{ZnO} = DEZ pulse / N₂ purge / H₂O pulse / N₂ purge ; n = 44 ; n₁ = 10) and ZnO würtzite

reference diffraction pattern (JCPDS 36-1451)

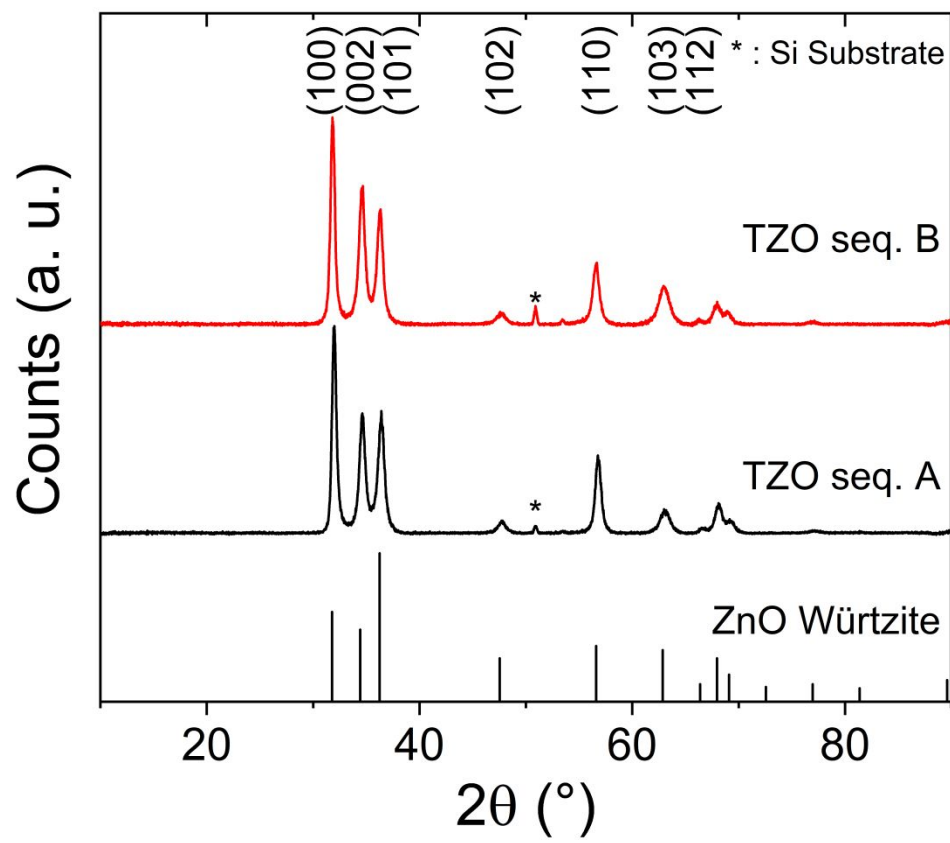


Figure S2. Influence of the cycle ratio $\{\text{TiO}_2\}:\{\text{ZnO}\}$ on the TZO film thickness as

determined by ellipsometry (full triangle) and XRR (cross) (sequence A, $n = 22 - 445$).

The thickness values expected from the linear combination of $\text{GPC}_{\text{TiO}_2}$ and GPC_{ZnO} are

presented by circles. The GPC values ($\text{GPC}_{\text{TiO}_2}$, GPC_{ZnO}) have been calculated from film

thicknesses determined by XRR.

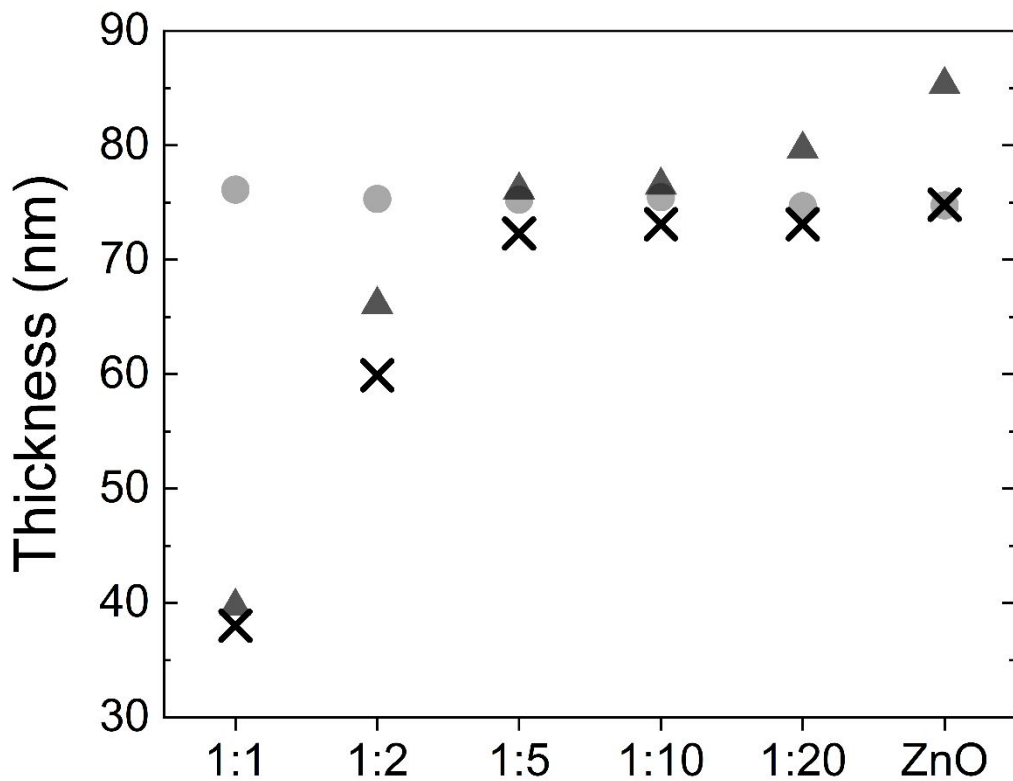


Figure S3. Influence of the cycle ratio $\{\text{TiO}_2\}:\{\text{ZnO}\}$ on the TZO structural properties (sequence A, $n = 22 - 445$) and reference diffraction patterns of ZnTiO_3 (JCPDS 26-1500), ZnO würtzite (JCPDS 36-1451), and anatase TiO_2 (JCPDS 20-1272)

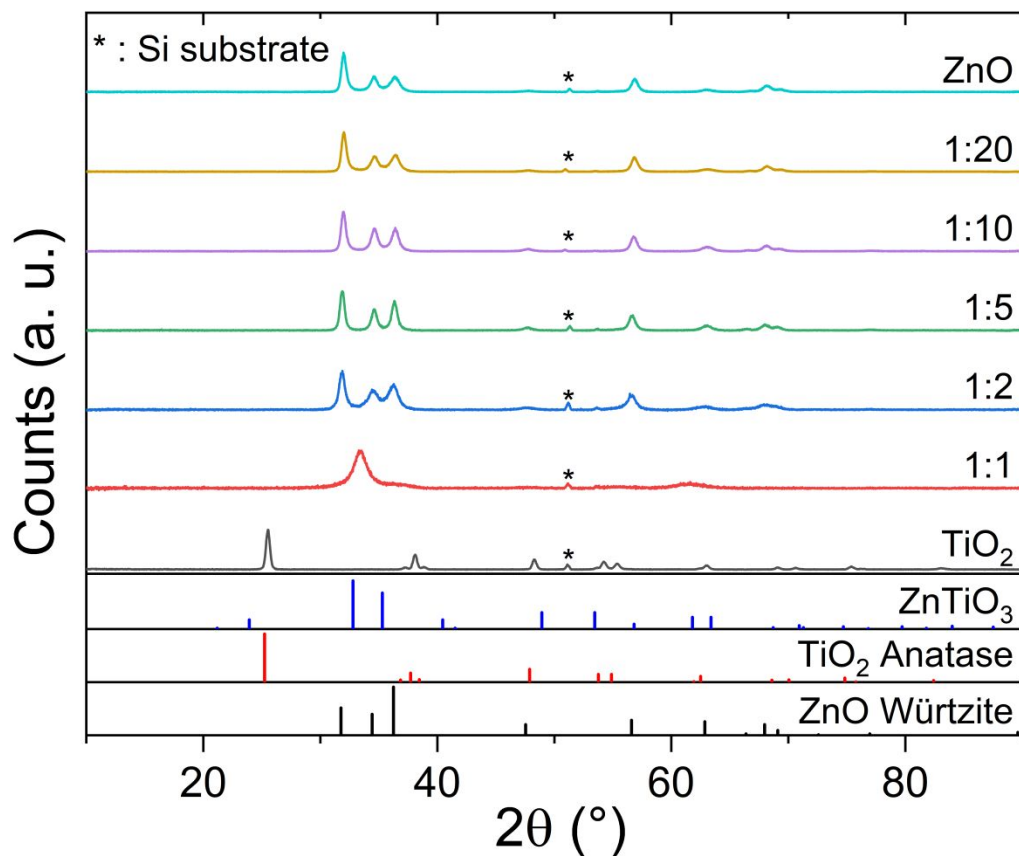


Figure S4. Influence of the cycle ratio $\{\text{TiO}_2\}:\{\text{ZnO}\}$ on the TZO optical properties
(sequence A, $n = 22 - 445$, transmission (solid lines, in %), reflection (dotted lines, in %))

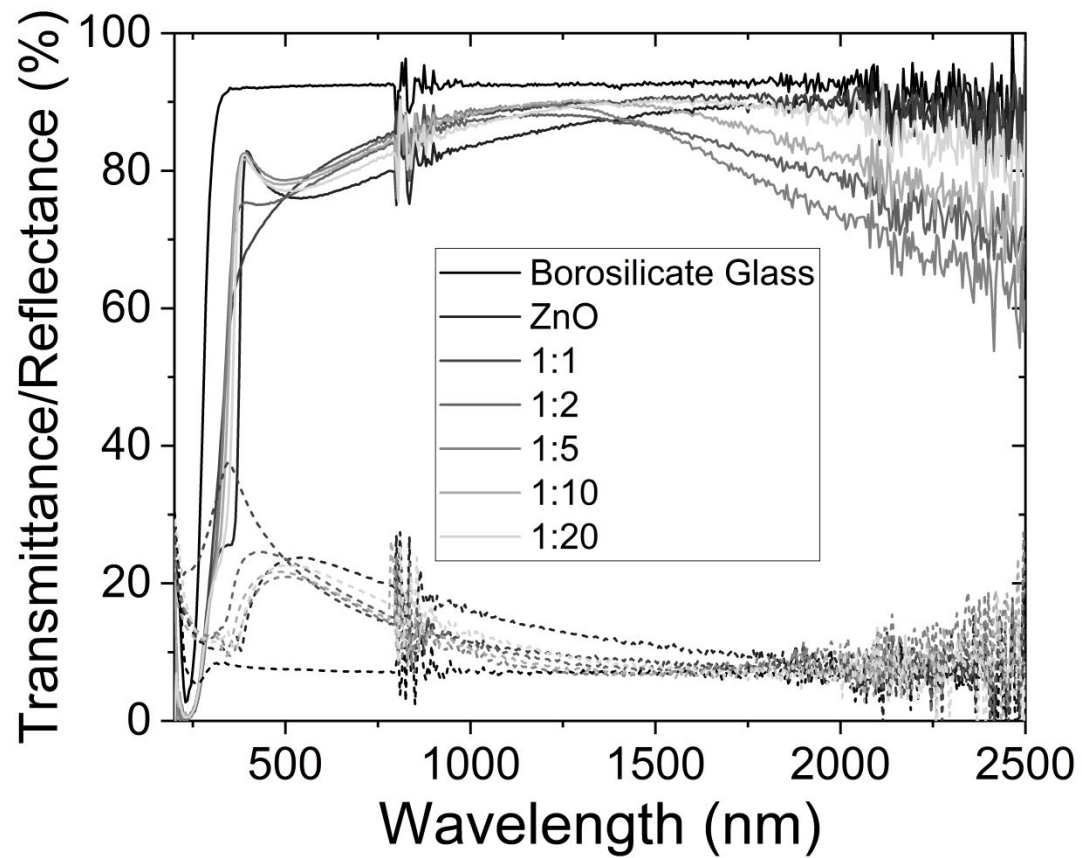


Figure S5. Influence of the cycle ratio $\{\text{TiO}_2\}:\{\text{ZnO}\}$ on the TZO index of refraction n at 633 nm

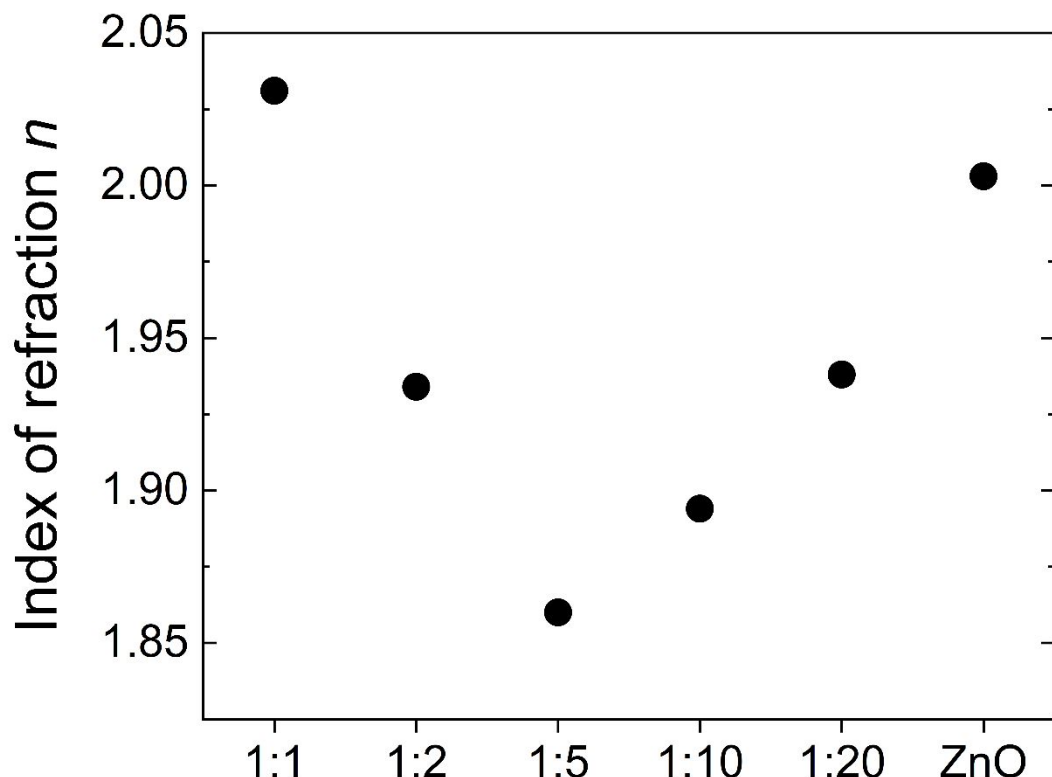


Figure S6. Influence of the cycle ratio $\{\text{TiO}_2\}:\{\text{ZnO}\}$ on the TZO electrical properties :

carrier concentration (diamonds, in cm^{-3}), mobility (squares, in $\text{cm}^2/\text{V} \cdot \text{s}$) and resistivity (triangles, in $\Omega \cdot \text{cm}$) (sequence A, $n = 22 - 445$)

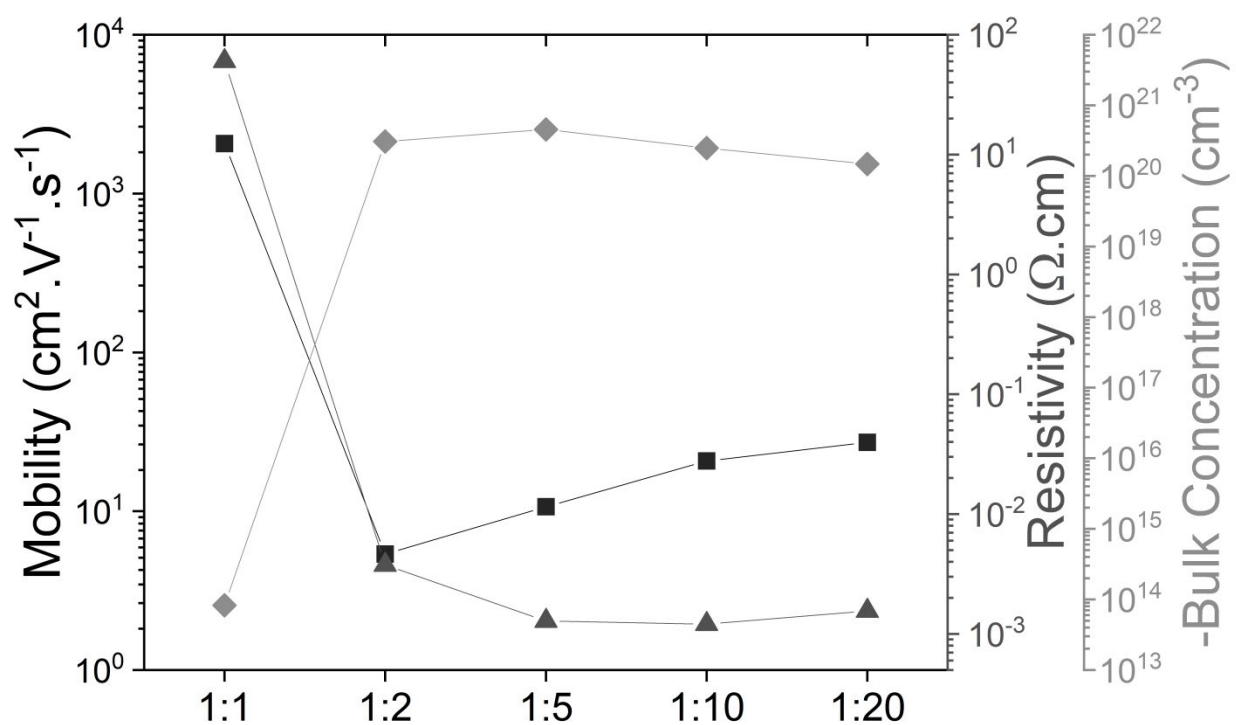


Figure S7. Influence of the film thickness on the TZO structural properties (sequence A, $n_1 = 10$) and reference diffraction patterns of ZnO würtzite (JCPDS 36-1451), and anatase TiO_2 (JCPDS 20-1272)

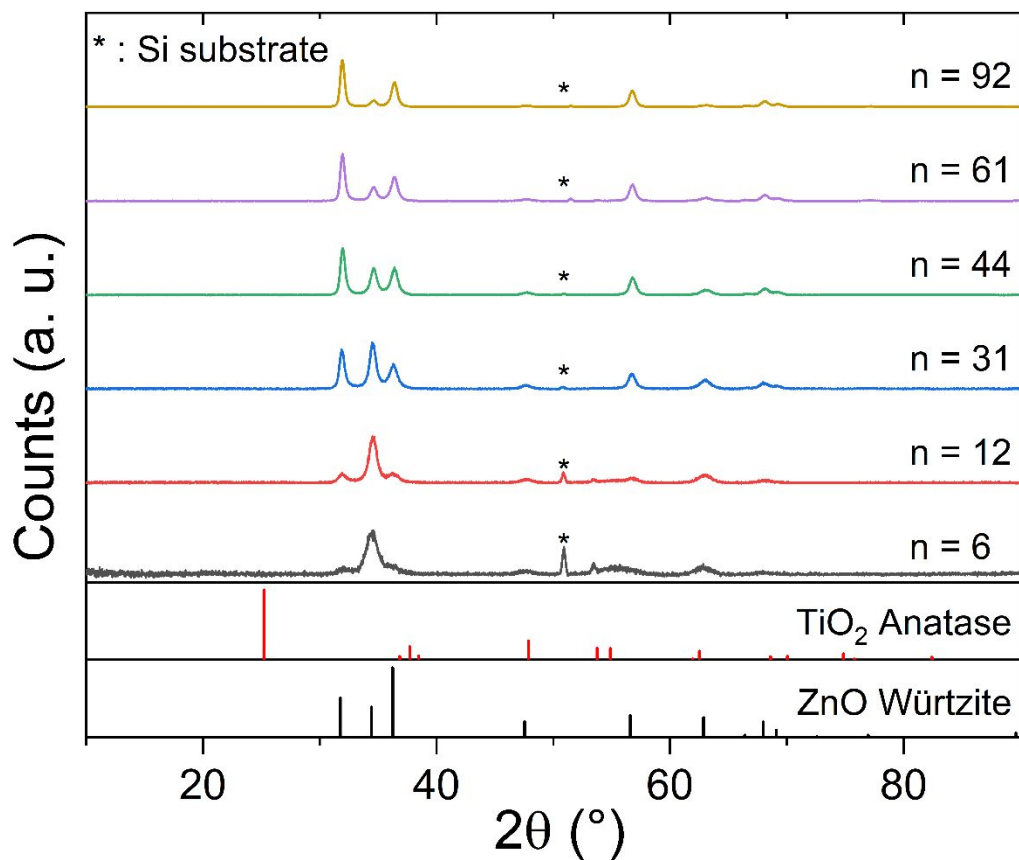


Figure S8. Influence of the film thickness on the TZO optical properties (sequence A, $n_1 = 10$, transmission (solid lines, in %), reflection (dotted lines, in %)

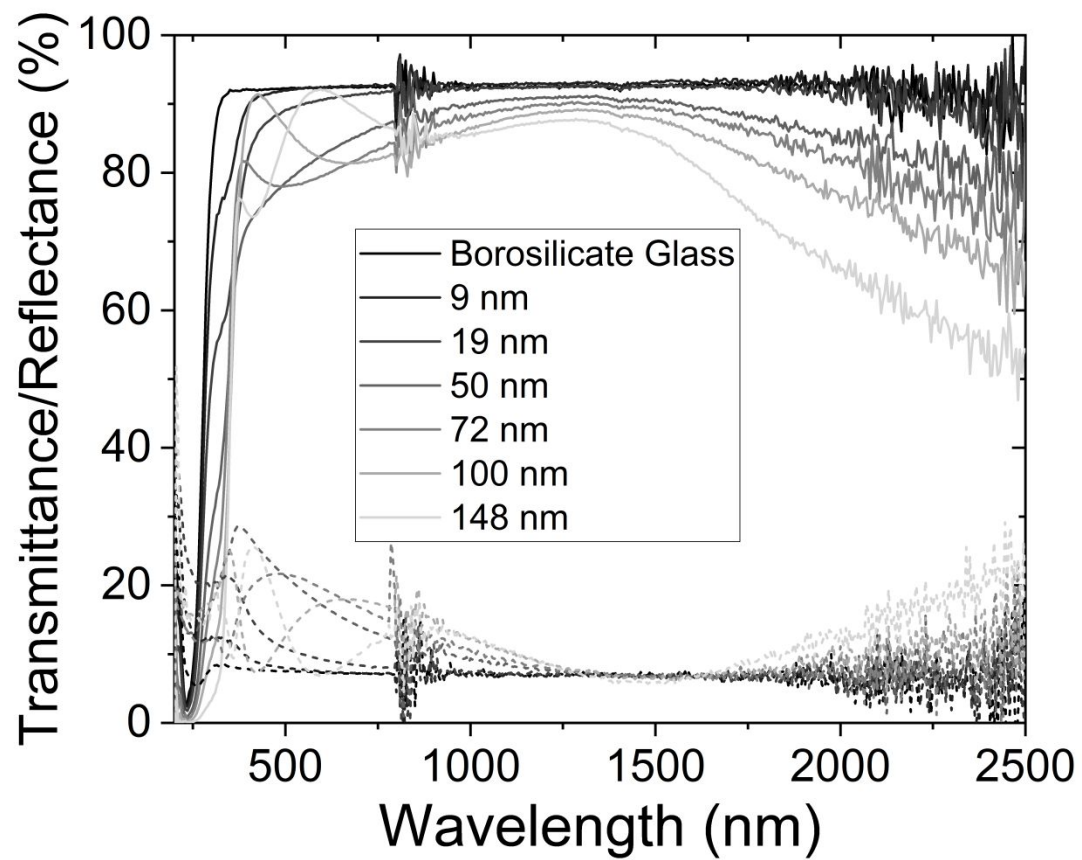


Figure S9. Influence of the film thickness on the TZO electrical properties: carrier concentration (diamonds, in cm^{-3}), mobility (squares, in $\text{cm}^2/\text{V} \cdot \text{s}$) and resistivity (triangles, in $\Omega \cdot \text{cm}$) (sequence A, $n_1 = 10$).

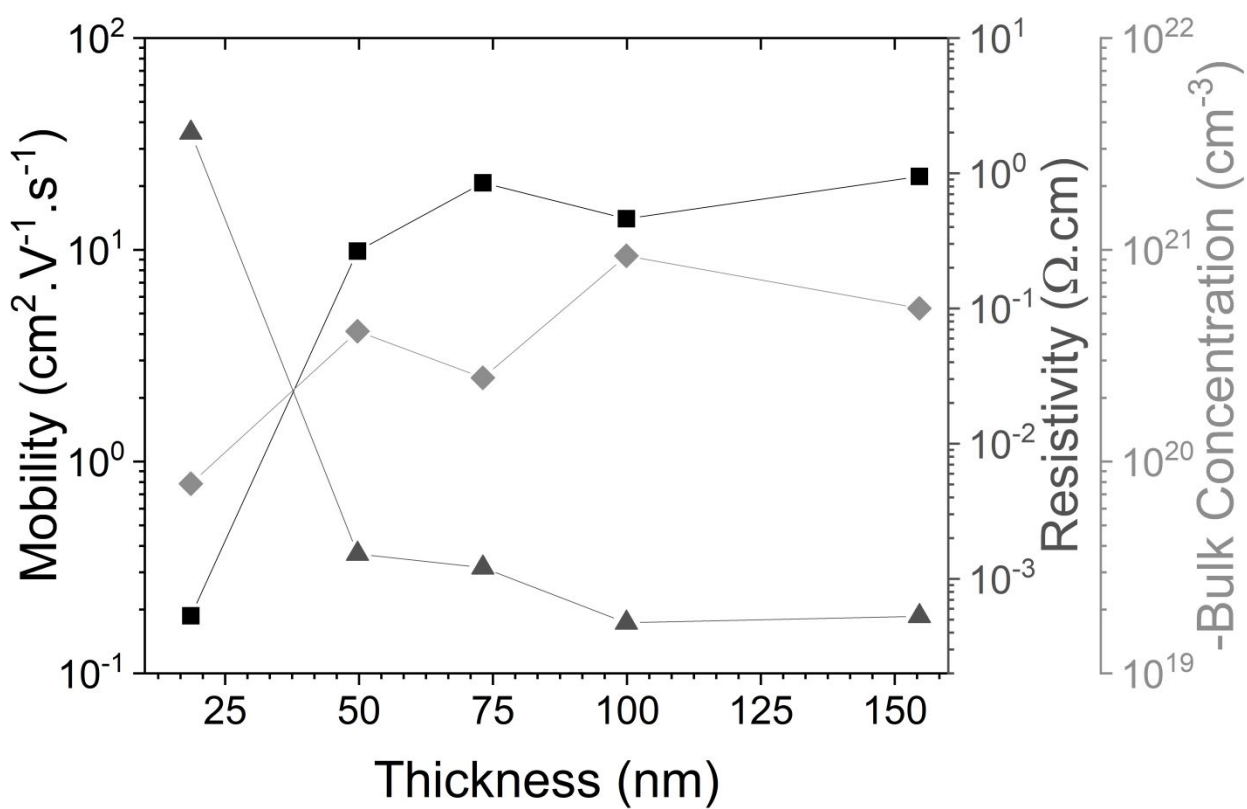


Figure S10. Cross sectional SEM image of the radial NW structure with ITO top electrode (by sputtering).

